Plant Physiol. (1987) 83, 97–104
0032-0889/87/83/0097/08/$01.00/0

The Path of Carbon Flow during NO_3^--Induced Photosynthetic Suppression in N-Limited *Selenastrum minutum*[1]

Received for publication May 6, 1986 and in revised form July 1, 1986

IVOR R. ELRIFI AND DAVID H. TURPIN*
Department of Biology, Queen's University, Kingston, Ontario, Canada K7L 3N6

ABSTRACT

Nitrate addition to nitrate-limited cultures of *Selenastrum minutum* Naeg. Collins (Chlorophyta) resulted in a 70% suppression of photosynthetic carbon fixation. In $^{14}CO_2$ pulse/chase experiments nitrate resupply increased radiolabel incorporation into amino and organic acids and decreased radiolabel incorporation into insoluble material. Nitrate resupply increased the concentration of phosphoenolpyruvate and increased the radiolabeling of phosphoenolpyruvate, pyruvate and tricarboxylic acid cycle intermediates, notably citrate, fumarate, and malate. Furthermore, nitrate also increased the pool sizes and radiolabeling of most amino acids, with alanine, aspartate, glutamate, and glutamine showing the largest changes. Nitrate resupply increased the proportion of radiolabel in the C-4 position of malate and increased the ratios of radiolabel in aspartate to phosphoenolpyruvate and in pyruvate to phosphoenolpyruvate, indicative of increased phosphoenolpyruvate carboxylase and pyruvate kinase activities. Analysis of these data showed that the rate of carbon flow through glutamate (10.6 μmoles glutamate per milligram chlorophyll per hour) and the rate of net glutamate production (7.9 μmoles glutamate per milligram chlorophyll per hour) were both greater than the maximum rate of carbon export from the Calvin cycle which could be maintained during steady state photosynthesis. These results are consistent with the hypothesis that nitrogen resupply to nitrogen-limited microalgae results in a transient suppression of photosynthetic carbon fixation due, in part, to the severity of competition for carbon skeletons between the Calvin cycle and nitrogen assimilation (IR Elrifi, DH Turpin 1986 Plant Physiol 81: 273–279).

NH_4^+ addition to N-sufficient microalgae and higher plant chloroplast, cell, or leaf disc preparations causes an increase in the proportion of ^{14}C incorporated into amino and organic acids (11, 13, 17, 20, 21). Both PEP[2] carboxylase and pyruvate kinase function as key enzymes in regulating carbon flow to amino acid synthesis (9, 21). During NH_4^+ resupply carbon skeletons from the Calvin cycle, starch or sucrose metabolism serve as sources of anaplerotic substrates for increased tricarboxylic acid cycle activity to produce keto-acids for amino acid synthesis (1, 9, 16). In these studies the total rate of ^{14}C incorporation into acid stable products remained unchanged following NH_4^+ enrichment (8, 17, 21) or in some cases increased (6, 12, 13, 20, 30).

In contrast, NO_3^- or NH_4^+ enrichment to N-limited *Selenastrum minutum* Naeg. Collins results in a transient suppression of photosynthetic carbon fixation that is characteristic of many species of N-limited microalgae (5, and references therein). We have proposed that N-induced photosynthetic suppression is the result of a competition for metabolites between the Calvin cycle and nitrogen assimilation (5). A rapid depletion of Calvin cycle intermediates following either NO_3^- and NH_4^+ resupply would contribute to the observed decrease in the rate of RuBP regeneration thus limiting photosynthetic carbon fixation (5).

If this model is correct, during NO_3^--induced photosynthetic suppression there should be a redirection of recently fixed photosynthate from starch and sucrose to amino acids. Furthermore, the rate at which carbon is required by amino acid synthesis should exceed the rate of TP export from the chloroplast which could be maintained during steady state photosynthesis. The results presented here are in agreement with the current model of N-induced photosynthetic suppression in *S. minutum* (5).

MATERIALS AND METHODS

Chemostat Culture. *Selenastrum minutum* Naeg. Collins, a green alga, was grown axenically under NO_3^--limitation in chemostat culture at a growth rate of 0.3 d^{-1} (18% of the maximal growth rate). Culture conditions were as previously described (5) with the exception that the inflow medium was supplied with 1 mM $NaNO_3$ and 300 μM K_2HPO_4, ensuring NO_3^- limitation. This resulted in steady state cell densities of 1.72 μg Chl·ml^{-1}.

Pulse/Chase Experiments. In these experiments, cells were harvested from chemostats and concentrated to approximately 43 μg Chl·ml^{-1} by gentle centrifugation (5000*g*, 5 min). Cells were placed in a water-jacketed cuvette (20°C) illuminated with two Kodak 600H projectors. DIC ($NaHCO_3$) was added to 1 mM and cells were preadapted for 15 min under these conditions. Following this preincubation period, DIC was measured and $H^{14}CO_3^-$ (7.27 μCi·$nmol^{-1}$, Atomic Energy Commission of Canada) was immediately added to the experimental cuvette. After a 10 s exposure, the $H^{14}CO_3^-$ was 'chased' by flooding the cuvette with 500 mM $NaH^{12}CO_3$. The culture pH did not change during the chase period. Samples (3 ml) were removed from the experimental cuvette at several time intervals, rapidly filtered onto illuminated 2.5 cm 934-AH glass-fiber filters (Whatman) and placed in 10 ml of kill solution (80% aqueous ethanol, 5% HCOOH). Samples were then homogenized and centrifuged to remove insoluble material. The supernatant, termed the crude algal extract, was evaporated to dryness, resuspended in 1.0 ml distilled H_2O and fractionated for amino acid and organic acid analysis as described below. At each sample time, additional aliquots (300 μl) were removed from the experimental cuvette and placed directly into 500 μl of kill solution. These were evaporated to dryness, resuspended in 1 ml H_2O and total acid

[1] Supported by the Faculty of Graduate Studies and Research of Queen's University and the Natural Sciences and Engineering Research Council of Canada.

[2] Abbreviations: PEP, phosphoenolpyruvate; TP, triose phosphate; mal, malate; fum, fumarate; cit, citrate; α-KG, α-ketoglutarate; RuBP, ribulose bisphosphate; GOGAT, glutamine 2-oxoglutarate aminotransferase (EC 2.6.1.53); GS, glutamine synthetase (EC 6.3.1.2); DIC, dissolved inorganic carbon; μ, growth rate; OAA, oxaloacetate; pyr, pyruvate.

stable radioactivity assessed by liquid scintillation counting (5).

Fractionation of Metabolites from Crude Algal Extracts. The water soluble portion of the crude algal extract was separated into acidic, basic, and neutral fractions by an ion-exchange procedure (4). Samples were applied to a DOWEX AG 50W-X8 column (1 cm^3) and rinsed with 20 ml H_2O to remove acidic and neutral species. The basic (amino acid) fraction was eluted with 20 ml of 2 N HCl, the eluant was evaporated to dryness and resuspended in 1 ml H_2O. Subsequent amino acid separations were as described below. The acidic and neutral fraction was applied to a DOWEX AG 1-X8 column (1 cm^3). Sugars were eluted with 20 ml H_2O. Organic acids were eluted with 7 ml 50% HCOOH, evaporated to dryness, and resuspended in 1 ml H_2O. Subsequent organic acid separations were as described below. P-esters were then eluted from the AG 1-X8 column with 15 ml of 2 N HCl. Incorporation of radiolabel was assessed for each total fraction.

Separation of Amino and Organic Acids. Amino acid samples (400 μl) were separated by ion-exchange HPLC (4). Recovery of amino acids ranged between 74 and 90% based on the recovery of an internal standard (α-aminoadipic acid). Incorporation of radiolabel into amino acids was measured by liquid scintillation counting of fractions collected during each amino acid run (4).

Organic acids were separated by isocratic HPLC using an Interaction ORH801 ion exclusion column. The mobile phase was 0.05 N H_2SO_4, the column temperature was 38°C and the flow rate was 0.8 $ml \cdot min^{-1}$. Organic acid samples (800 μl) were detected by UV absorbance at 210 nm. Incorporation of radiolabel into organic acids was measured by liquid scintillation counting of fractions collected during each organic acid run (20 min).

Decarboxylation of Malate. Malate was assayed for radiolabel in the C-4 position by decarboxylation with NADP malic enzyme (EC 1.1.1.40, Sigma Chemical Co.) using a modification of the method of Rutter and Lardy (24). Aliquots (30 μl) of each total organic acid fraction were added to 1 ml of reaction assay buffer (20 mM Hepes [pH 7.5], 5 mM cysteine, 10 mM $MgCl_2$, 1 mM $NADP^+$) and the reaction was initiated by addition of 0.5 units of enzyme. After 1 h the vials were acidified with kill solution, evaporated to dryness and the remaining radioactivity assessed by liquid scintillation counting. Assay efficiency was estimated at 84% using a standard of C-4 labeled malate.

Ninhydrin Decarboxylation of Amino Acids. The proportion of label in the α-carboxyl position of amino acids was determined using a modification of the ninhydrin decarboxylation method of Greenberg and Rothstein (7). Aliquots (100 μl) of each total amino acid fraction were added to 750 μl of reaction assay buffer (0.5 M citrate [pH 2.5]) and the reaction was initiated by addition of 750 μl methyl cellosolve in the presence or absence of 0.28 M ninhydrin. Samples were incubated for 20 min in a boiling water bath (96°C), cooled to room temperature, and the remaining radioactivity assessed by liquid scintillation counting. Assay efficiency was estimated at 93% using a standard of [1-^{14}C]glycine. Loss of radiolabel from positions other than the α-carboxyl carbon was insignificant (8%) using a standard of [2-^{14}C]glycine.

RESULTS

Effects of NO_3^- Addition on ^{14}C Incorporation. During the 10 s $H^{14}CO_3^-$ exposure control cells accumulated 50.1 nmol $C \cdot mg^{-1}$ Chl, while NO_3^- enriched cells accumulated 18.1 nmol $C \cdot mg^{-1}$ Chl. Total radiolabel recovery was unchanged over the duration of the experiment. The rates of gross carbon fixation calculated from these data were 18.0 and 6.5 $\mu mol\ CO_2 \cdot mg^{-1}$ $Chl \cdot h^{-1}$ for control and N pulsed cells, respectively. This represented a 64% NO_3^--induced suppression of photosynthetic carbon fixation.

In control cells, 77% of total acid stable radiolabel remained in the soluble fraction after 30 s. This declined to 24% after 61 min (Fig. 1A). In cells resupplied with NO_3^-, 100% of the total acid stable counts remained in the soluble fraction after 30 s, declining to 35% after 61 min (Fig. 1A). A greater percentage of the total acid stable counts were incorporated into amino and organic acids when cells were resupplied with NO_3^- (Fig. 1, B and C). Over the duration of the experiment, incorporation of radiolabel into amino acids accounted for between 22 to 8% and 31 to 13% of the total acid stable counts in control and NO_3^- enriched cells, respectively (Fig. 1B). Similarly, over the duration of the experiment, incorporation of radiolabel into organic acids accounted for between 44.5 to 12.5% and 65.1 to 19.9% of the total acid stable counts in control and NO_3^- enriched cells, respectively (Fig. 1C). Cells resupplied with NO_3^- incorporated

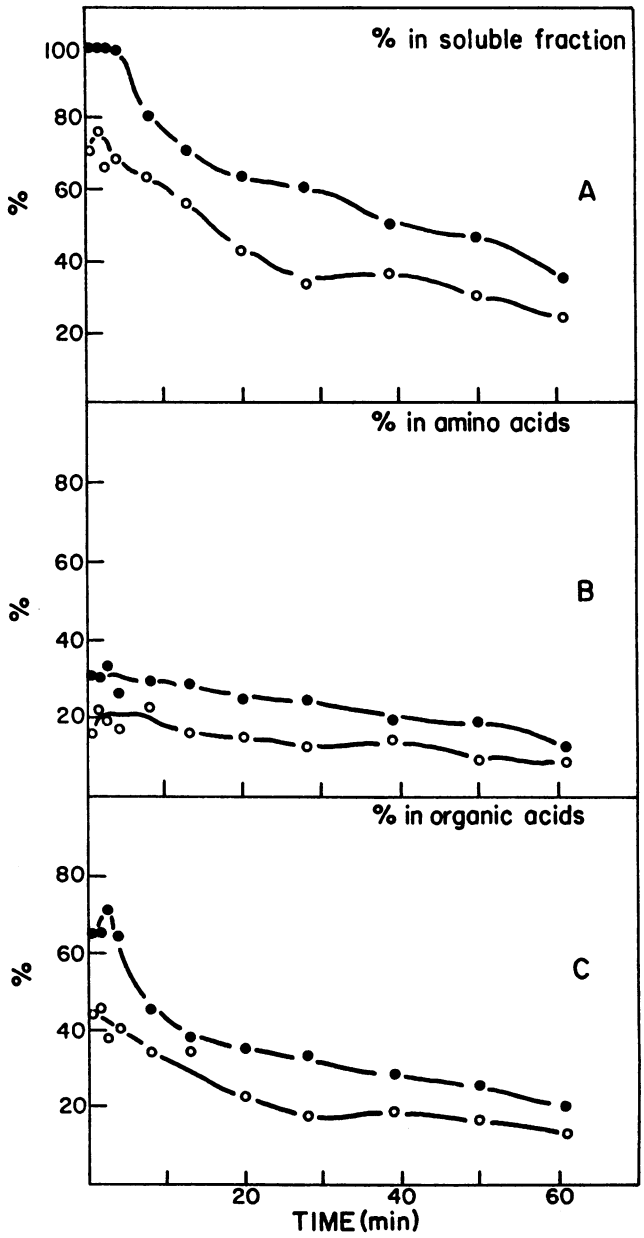

FIG. 1. The recovery of radiolabel following a 10 s exposure to $H^{14}CO_3^-$ as a percent of the total acid stable counts in the total soluble fraction, amino acids, and organic acids. (○), control; (●), NO_3^- enriched. A, Recovery of acid stable counts in soluble material; B, recovery of acid stable counts in amino acids; C, recovery of acid stable counts in organic acids.

2.7 times less radiolabel into sugars. Radiolabel incorporation into P-esters represented less than 7% of the total acid stable counts and was apparently not affected by NO_3^- resupply (data not shown).

Effects of NO_3^- Addition on Amino Acids. In the absence of resupplied NO_3^-, Glu comprised the greatest proportion of amino nitrogen (620 nmol·mg^{-1} Chl, 68% of total amino N). Other amino acids present as a significant proportion of amino nitrogen were Asp, Ala, and Gln, at 4.0, 4.0, and 5.0%, respectively (Fig. 2, A–D). The contribution of all other amino acids in total was never more than 26% of total amino N. In control cells, the pool sizes of most amino acids decreased over the duration of the experiment due to an increase in the severity of N starvation (Fig. 2, A–D). Upon N resupply, the pool sizes of most amino acids increased (Fig. 2, A–D; Table I). Following NO_3^- resupply, 92% of amino nitrogen was present in Ala, Asp, Glu, and Gln, with 83% of total amino nitrogen being present in Glu. The flux of radiolabel into amino acids was represented as the percent of the total radiolabel incorporation which appeared in each amino acid. These values increased in response to NO_3^- resupply (Fig. 2, E–H; Table I). The largest increases were seen in Asp, Glu, Gln, and Gly (Fig. 2, E–H; Table I). The same trends were evident when these results were expressed as a percentabe of the total radiolabel in the amino acid fraction (Table I). NO_3^- addition caused major changes in the specific activities of Ala and Gln (Fig. 2, J and L; Table I). Immediately following N enrichment, the specific activity of Ala decreased from the control value of 273 pmol C·nmol^{-1} to 102 pmol C·nmol^{-1} (Fig. 2J). The specific activity of Gln exhibited a transient increase, followed by a decrease to control levels (Fig. 2L). The specific activities of Asp and Glu increased slightly following N resupply but declined to approximately one-tenth the specific activity in control unenriched cells after 60 min (Fig. 2, I and K). In control cells, decarboxylation of amino acids with ninhydrin resulted in loss of 86 to 94% of the radiolabel in the amino acid fraction (Fig. 3). In cells resupplied with NO_3^- a greater proportion of radiolabel remained in amino acids following treatment with ninhydrin (Fig. 3). This demonstrated that following NO_3^- resupply more radiolabel was found in positions other than the α-carboxyl carbon.

Effects of NO_3^- Addition on PEP Pool Size and Radiolabel. The pool size of PEP increased from 200 nmol·mg^{-1} Chl to 700 nmol·mg^{-1} Chl within 10 min of NO_3^- resupply and then declined to control values within 20 min (Fig. 4A). Initially there was an increase in the total acid stable radiolabel incorporated into PEP in response to N resupply but this label moved rapidly out of PEP during the chase period (Fig. 4B). The specific activity of PEP decreased approximately 3-fold in response to N resupply (Fig. 4C).

Effects of NO_3^- Addition on Organic Acids. The flux of radiolabel into organic acids was represented as the percent of the total radiolabel incorporation which appeared in each organic acid. The proportion of radiolabel incorporated into organic acids increased in response to NO_3^- resupply. The largest increases were seen in citrate, cis-aconitate, pyr, mal, and fum, while radiolabel incorporation into succinate did not change following NO_3^- resupply (Fig. 5; Table II). Similar trends were seen when radiolabel incorporation was expressed as a percentage of the total organic acid incorporation. In NO_3^- enriched cells, after 30 s the greatest proportion of radiolabel was found in malate but after 20 min pyr contained the greatest proportion (Table II). In control cells, decarboxylation with NADP malic enzyme resulted in little or no detectable loss of radiolabel (Fig. 6A). In cells resupplied with NO_3^-, this treatment resulted in a 30% loss of ^{14}C. This loss could account for most of the radiolabel in malate, indicating a major increase in C-4 radiolabeling of mal following NO_3^- resupply (Fig. 6B).

DISCUSSION

Flow of Carbon During N-Induced Photosynthetic Suppression. We have shown that N resupply to N-limited *S. minutum* can result in conditions where photosynthetic carbon fixation is RuBP-limited. We suggest that this is a result of rapid depletion of Calvin cycle intermediates for use in N assimilation (5). If this hypothesis were correct we would predict that during ^{14}C pulse/chase experiments (a) there would be an increase in glycolytic activity, (b) there would be an increase in the activities of PEP carboxylase and pyr kinase, (c) there would be an increase in

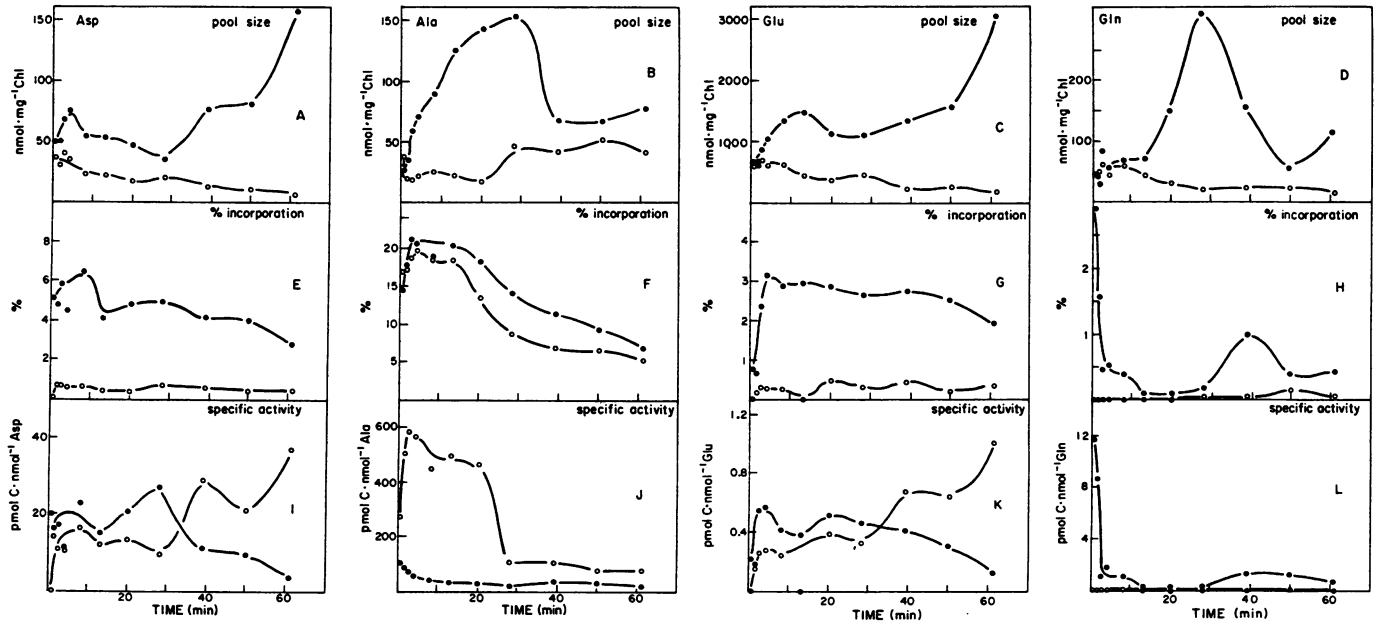

FIG. 2. The pool sizes (panels A, B, C, D), radiolabel incorporation as a percent of the total acid stable counts (panels E, F, G, H) and specific radioactivities (panels I, J, K, L) of the amino acids Asp (panels A, E, I), Ala (panels B, F, J), Glu (panels C, G, K), and Gln (panels D, H, L) following a 10 s exposure to $H^{14}CO_3^-$. (O), control; (●), NO_3^- enriched.

Table I. *Amino Acid Pool Sizes and Radiolabel Incorporation as a Percent of the Total Acid Stable Counts in Control and NO_3^- Enriched Cells 20 Min after a 10 s Exposure to $H^{14}CO_3^-$*

	Pool Size				Radiolabel			
	Amino acid mg^{-1} Chl		% of total amino acid		% of total ^{14}C		% of amino acid ^{14}C	
	−N	+N	−N	+N	−N	+N	−N	+N
	nmol							
Ala	17.9	143.8	2.8	8.8	13.46	18.40	88.4	66.4
Asn	23.2	45.3	3.7	2.8	<0.002	<0.002	<0.01	<0.01
Asp	17.1	35.3	2.7	2.9	0.37	4.83	2.4	17.4
Glu	371.5	1119.6	58.4	68.4	0.46	2.88	3.1	10.4
Gln	32.4	148.5	5.1	9.1	<0.002	0.32	<0.01	1.1
Gly	111.3	39.8	17.5	2.4	<0.002	0.45	<0.01	1.6
Ser	43.2	58.5	6.8	3.6	0.93	1.17	6.1	4.2
Thr	19.4	35.1	3.1	2.1	<0.002	<0.002	<0.01	<0.01

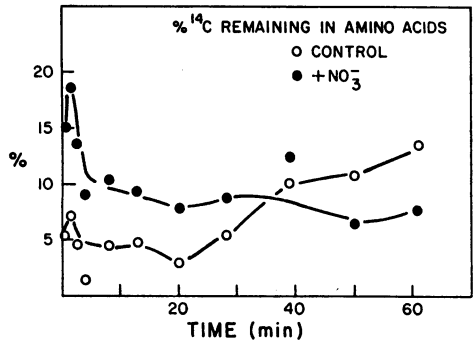

FIG. 3. The percent of radiolabel remaining in amino acids following decarboxylation with ninhydrin as a percent of the total radiolabel incorporated into amino acids. (O), control; (●), NO_3^- enriched.

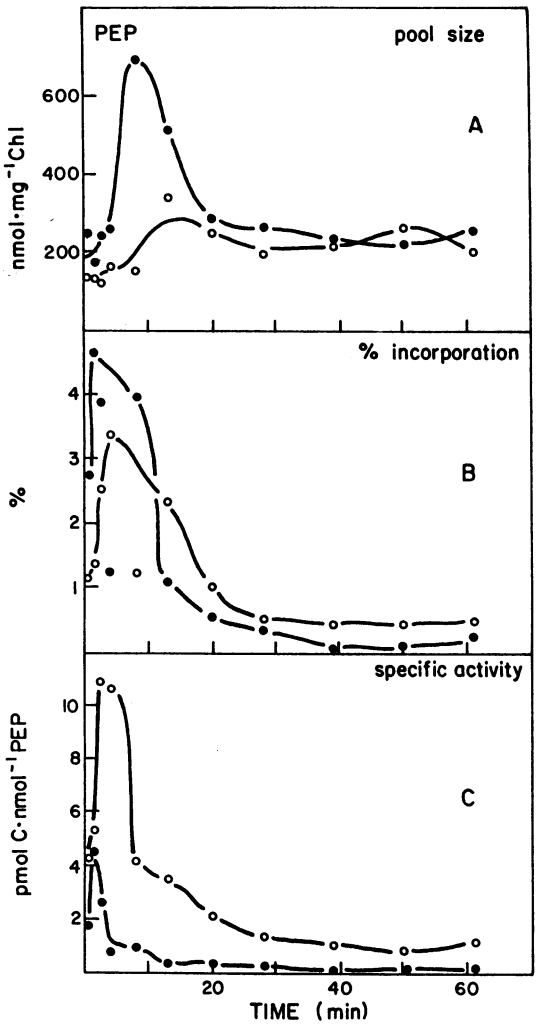

FIG. 4. The pool size, radiolabel incorporation as percent of the total acid stable counts and specific radioactivity of PEP following a 10 s exposure to $H^{14}CO_3^-$. (O), control; (●), NO_3^- enriched. A, The pool size of PEP; B, the percent of radiolabel incorporated into PEP; C, the specific activity of PEP.

tricarboxylic acid cycle activity in support of N assimilation, and (d) the rate at which triose-P was exported from the Calvin cycle in support of amino acid synthesis would exceed the maximum sustainable rate allowing for the maintenance of steady state carbon fixation.

Increased Glycolytic Activity Following N Resupply. Redirection of photosynthetic carbon flow to amino acids requires glycolytic activity to provide anaplerotic substrates for the tricarboxylic acid cycle. The increases in PEP concentration and radiolabeling in response to N resupply are consistent with increased flow of recent photosynthate through glycolysis (Fig. 4).

Increased PEP Carboxylase Activity. In order to maintain tricarboxylic acid cycle integrity following NO_3^- resupply, an increase in PEP carboxylase activity would be required. Following NO_3^- resupply there was an increase in the radiolabel present in malate (Fig. 5B). If this radiolabel were due to PEP carboxylase activity, then radiolabel would be preferentially located in the C-4 position, since OAA and mal rapidly equilibrate due to the reversibility of the mal dehydrogenase reaction (29). Decarboxylation with NADP malic enzyme revealed that most of the radiolabel in mal was in the C-4 position following NO_3^- resupply, in contrast with control cells (Fig. 6). This observation strongly suggests increased PEP carboxylase activity. OAA is the four carbon keto-acid precursor for Asp synthesis. Following NO_3^- resupply, there was a large increase in both the pool size and the proportion of radiolabel in Asp (Fig. 2, B and F), reflecting increased OAA synthesis and thus increased PEP carboxylase activity. In addition, the higher specific activity of Asp compared to PEP reflected additional flux of radiolabel into OAA and Asp through PEP carboxylase (Figs. 2J; 4C). The Asp:PEP ratio increased by up to 56-fold following NO_3^- resupply (Fig. 7B). Increases in the Asp:PEP ratio have previously been interpreted as reflecting increased PEP carboxylase activity (20). Justification for the usefulness of this ratio is based on the reversibility of the transamination reaction between OAA and Asp (20). Data presented here are consistent with previous work that has shown the importance of N in stimulating dark carbon fixation (5, 12, 27).

Increased Pyruvate Kinase Activity. Increased pyr kinase activity would also be predicted if the proposed path of carbon flow were correct. Consistent with this prediction, NO_3^- resupply increased radiolabel incorporation into pyr (Fig. 5A). In addition, the pool size and radiolabel incorporation into Ala increased in response to NO_3^- enrichment. This would be expected if pyr kinase were stimulated since pyr is the immediate carbon precursor for Ala synthesis. There was also an increase in the pyr:PEP ratio of as much as 22-fold following NO_3^- resupply (Fig. 7C). Increases in the pyr:PEP radiolabel ratio have been interpreted as reflecting increased carbon flux through PEP to pyr since the conversion of PEP to pyr is a rate limiting metabolic step (9, 11, 12, 17, 20, 21).

Increased Tricarboxylic Acid Cycle Activity. The preceding

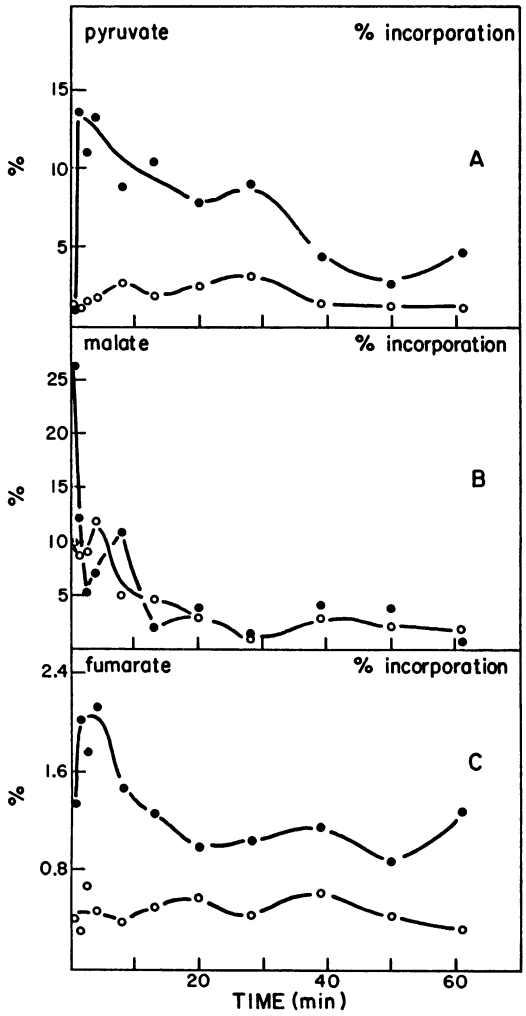

FIG. 5. The incorporation of radiolabel into organic acids as a percent of total acid stable counts following a 10 s exposure to $H^{14}CO_3^-$: A, pyruvate; B, malate; C, fumarate. (O), Control; (●), NO_3^- enriched.

results documented increased availability of anaplerotic substrates for the tricarboxylic acid cycle during N-induced photosynthetic suppression. Further evidence suggests that tricarboxylic acid cycle activity increased in response to NO_3^- enrichment. In particular, NO_3^- increased the incorporation of radiolabel into tricarboxylic acid cycle intermediates, notably cit, fum, and mal (Fig. 5; Table II). In addition, the mal:Asp ratio decreased as much as 22-fold following NO_3^- resupply (Fig. 7A). Decreases in the mal:aspartate ratio have been interpreted as reflecting an increase in tricarboxylic acid cycle activity (14). Finally, the Ala:pyr ratio decreased as much as 9-fold in response to NO_3^- resupply (Fig. 7D). We interpret this to reflect the increased flux of carbon from pyr to the tricarboxylic acid cycle to satisfy the α-KG demand from N assimilation. Consistent with this, Glu:pyr aminotransferase has been shown to be relatively unaffected by N concentration (23). Thus, following NO_3^- resupply the absolute carbon flux to Ala increased but relatively more pyruvate was diverted to Acetyl-CoA formation. These data are also consistent with previous studies that have shown that O_2 consumption and tricarboxylic acid cycle mediated CO_2 efflux in the light increase in response to N resupply (3, 5).

Consistent with previous reports, the major increases in amino N concentration and radiolabel incorporation were observed in Ala, Asp, Glu, and Gln (6, 9, 11–13, 15, 17, 20, 21, 27, 30). Glu comprised the greatest proportion of amino N in both control and NO_3^- enriched cells (Table I). Of the radiolabel in amino acids the greatest proportion was present in Ala, in both control and NO_3^- enriched cells (Fig. 1; Table I). This is similar to other data which indicate a direct flow of Calvin cycle carbon to Ala and other pyruvate-derived amino acids (25). Radiolabel incorporation and pool sizes of most other amino acids increased significantly following NO_3^- resupply, also indicating increased carbon flow into amino acids (Table I). In cells resupplied with NO_3^-, as much as 5 times more radiolabel remained associated with amino acids following decarboxylation with ninhydrin (Fig. 3). These data are interpreted as reflecting an increase in the randomization of radiolabel in amino acids through both an increase in flow of radiolabeled carbon from photosynthesis to amino acids and an increase in tricarboxylic acid cycle activity. Presumably this randomization is facilitated by fumarase. Results shown here for N-limited cells are consistent with previous results for N-sufficient cells (6, 8, 11–13, 17, 20, 21, 30).

Rates of Carbon Flux in Support of Amino Acid Synthesis. If the model for photosynthetic suppression is correct then the rate of carbon flow from the Calvin cycle into amino acids in response to N resupply should exceed that possible under conditions of steady state carbon fixation. The rates of photosynthesis calculated from the 10 s exposure to $H^{14}CO_3^-$ were 18.0 and 6.5 μmol $CO_2 \cdot mg^{-1}$ Chl $\cdot h^{-1}$ for control and NO_3^- enriched cells, respectively. Given these rates, and the stoichiometry presented in Elrifi and Turpin (5), the maximum possible rate of triose-P efflux from the plastid while maintaining steady state photosynthesis by control cells would be 6.0 μmol TP $\cdot mg^{-1}$ Chl $\cdot h^{-1}$. Assuming there was no starch or sucrose metabolism we calculate the maximum possible rate of α-KG removal at 3.0 μmol α-KG $\cdot mg^{-1}$ Chl $\cdot h^{-1}$. If our hypothesis is viable, then this rate must be

Table II. *Radiolabel Incorporation into Organic Acids as a Percent of the Total Acid Stable Counts and as a Proportion of the Total Radiolabel in the Organic Acid Fraction in Control and NO_3^- Enriched Cells 30 s and 20 min after a 10 s Exposure to $H^{14}CO_3^-$*

	30 s				20 min			
	% of total ^{14}C		% of organic acid ^{14}C		% of total ^{14}C		% of organic acid ^{14}C	
	−N	+N	−N	+N	−N	+N	−N	+N
cis-Aconitate	0.37	1.21	2.4	3.4	0.39	0.86	3.2	4.4
Citrate	0.39	1.33	2.6	3.7	0.76	2.10	6.2	10.8
Fumarate	0.40	1.34	2.6	3.8	0.58	1.01	4.7	5.2
Malate	9.85	26.34	64.4	73.9	2.81	3.79	22.9	19.5
Phosphoenolpyruvate	1.12	2.73	7.3	7.7	1.01	0.53	8.2	2.7
Pyruvate	1.22	1.13	8.0	3.2	2.51	7.86	20.5	40.6
Succinate	1.94	1.58	12.7	4.4	3.46	3.24	34.3	16.7

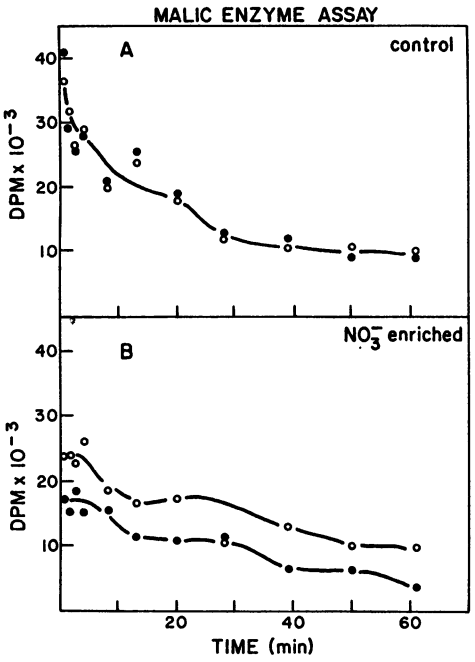

FIG. 6. The effect of NADP malic enzyme on recovery of radiolabel in organic acids. A, Control cells; (O), no enzyme; (●), enzyme added. B, NO_3^- enriched cells; (O), no enzyme; (●), enzyme added.

exceeded. Data presented here are consistent with this prediction. The rate of carbon flow between Glu and Gln was calculated by fitting curves to the pool size and radiolabel incorporation data (Fig. 2) and using the derivatives of these equations in equation 1.

$$dn/Dt = (dB^*/Dt - SA_b dB/Dt)/(SA_a - SA_b) \quad (1)$$

where dn/Dt is the rate of carbon flow between a and b, dB^*/Dt is the rate of radiolabel flux, dB/Dt is the rate of change in pool size, and SA is the specific activity.

Based on these calculations the rate of carbon flow through Glu into Gln increased from the control rate of 0.029 μmol amino acid·mg^{-1} Chl·h^{-1} to 10.6 μmol amino acid·mg^{-1} Chl·h^{-1} following NO_3^- resupply. Both the observed net rate of Glu production (7.9 μmol Glu·mg^{-1} Chl·h^{-1}) and the calculated rate of carbon flow through Glu (10.6 μmol Glu·mg^{-1} Chl·h^{-1}) following N resupply were greater than the maximum rate sustainable by carbon export from the chloroplast. Given the synthesis of amino acids other than Glu (Fig. 2), the actual carbon demand would have been far greater than could be supported during maintenance of steady state photosynthesis. This is consistent with the proposal that N-induced photosynthetic suppression is in part the result of triose P removal from the chloroplast at a rate too great to support steady state photosynthesis.

Stoichiometric considerations suggest that although the Calvin cycle is one source of carbon skeletons, starch breakdown must also be a major source of triose-P for N assimilation (5). Consistent with this, a greater proportion of the total acid stable counts were present in amino and organic acids following NO_3^- resupply with a corresponding decrease in the radiolabel present in insoluble material (Fig. 1). These data suggest that NO_3^- resupply diverted fixed carbon from starch biosynthesis to amino and organic biosynthesis, consistent with previous reports (1, 16). Furthermore, since the major source of carbon for N assimilation was starch breakdown, this hypothesis predicts a large flux of cold carbon through the tricarboxylic acid cycle and into amino acids. Consistent with this, the specific activities of Ala, Asp, Glu, Gln, and PEP decreased over the chase period following NO_3^- resupply (Figs. 2, I–L; 4C).

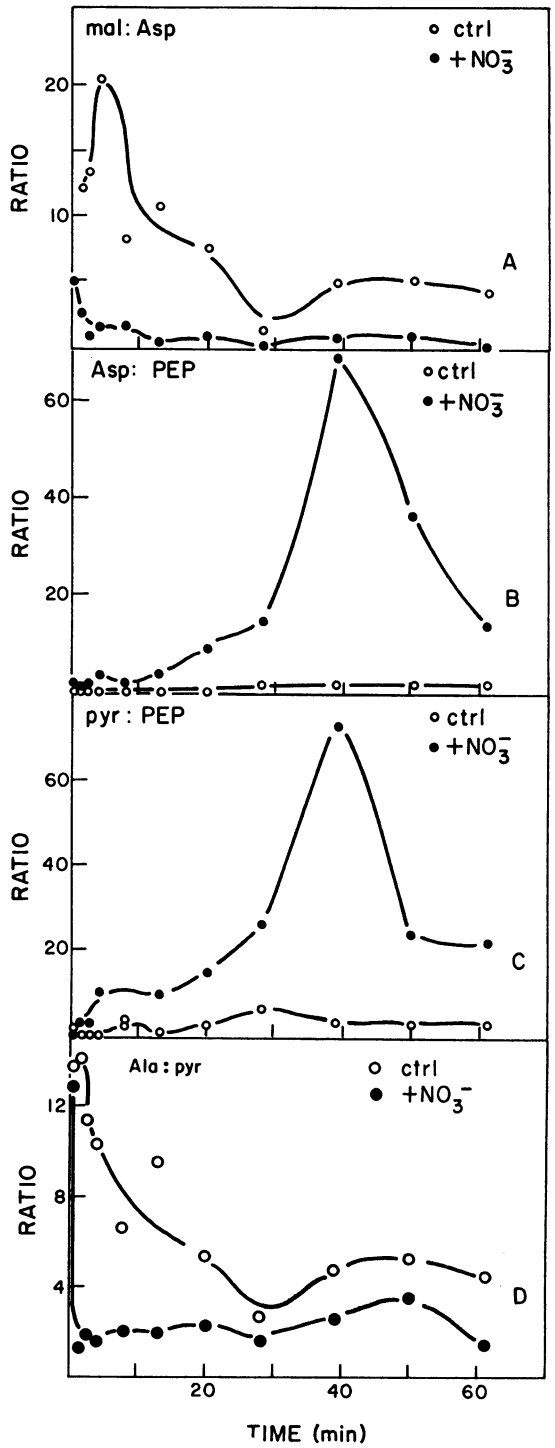

FIG. 7. The effect of NO_3^- enrichment on the ratios of total radiolabel incorporation following a 10 s exposure to $H^{14}CO_3^-$ for (A) mal:Asp, (B) Asp:PEP, (C) pyr:PEP, and (D) Ala:pyr. (O), Control; (●), NO_3^- enriched.

Regulation of N-Induced Changes in Photosynthetic Carbon Flow. Several mechanisms have been postulated to control the regulatory effects of N on photosynthetic carbon flow including cytoplasmic pH, energy charge, the Pi concentration and allosteric feedback (1, 9–11, 20, 22). Both Pi concentration and allosteric effectors are likely to be important in the regulation of photosynthetic carbon flow. One possible model implicates Pi as a key metabolite in the control of N-induced changes in photo-

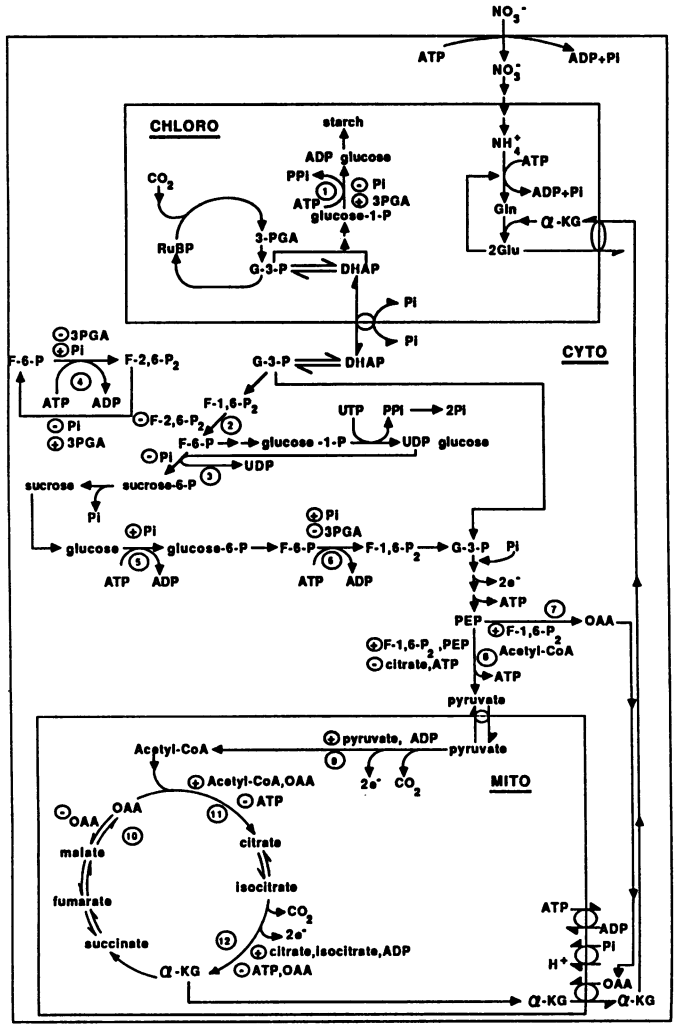

FIG. 8. A model for the mechanism of regulation of N-induced changes in photosynthetic carbon flow by the intracellular inorganic phosphate concentration. The key enzymes involved in the regulation of carbon flow from photosynthesis to amino acids are numbered. Positive effectors or activators of enzymes are indicated by the symbol (+), while negative effectors or inhibitors of enzymes are indicated by the symbol (−). (1), ADPglucose pyrophosphorylase; (2), cytosolic fructose-1,6-bisphosphatase; (3), sucrose phosphate synthase; (4), 2-phosphofructokinase; (5), hexokinase; (6), phosphofructokinase; (7), PEP carboxylase; (8), pyruvate kinase; (9), pyruvate dehydrogenase complex; (10), malate dehydrogenase; (11), citrate synthase; (12), isocitrate dehydrogenase.

synthetic carbon flow (Fig. 8). It is proposed that an N-induced increase in the cytosolic Pi concentration would stimulate the flow of carbon from photosynthesis to amino acids. An increase in cytosolic Pi concentration would inhibit sucrose phosphate synthase, fructose-1,6-bisphosphatase, and ADPglucose pyrophosphorylase, thereby decreasing flow of photosynthate to sucrose and starch synthesis. In addition, increased cytosolic Pi would stimulate hexokinase, phosphofructokinase, and TP export via the chloroplastic Pi translocator. This would increase synthesis of F-1, 6-P_2, increasing glycolytic activity and stimulating PEP carboxylase and pyr kinase activities, thereby providing an increased supply of pyr and OAA for the tricarboxylic acid cycle. Consequently there would be increased availability of α-KG for N assimilation.

Available evidence indicates Pi is potentially an important metabolite in carbon metabolism (22, 26, 28, 29). Increased intracellular Pi concentrations might be expected due to ATP hydrolysis as a result of rapid NO_3^- uptake and assimilation. In whole cells, ATP levels exhibit a transient decrease following N resupply (9, 10, 18, 19), but the intracellular stoichiometry of Pi is complex and it is unclear whether cytoplasmic Pi would increase or decrease in response to N enrichment. Increases in cytosolic Pi concentrations following N resupply would be consistent with Pi control of N-induced changes in photosynthetic carbon flow (Fig. 8).

CONCLUSIONS

In summary, the data presented here indicate a path of carbon flow from photosynthesis to amino acid synthesis similar to other reports (1, 2, 6, 9–12, 17, 20, 21). N enrichment results in diversion of photosynthetic carbon flow to glycolysis, the tricarboxylic acid cycle and subsequently into amino acids. We have shown that the rate of carbon flow from the Calvin cycle to N assimilation greatly exceeds the maximum rate sustainable if steady state photosynthesis is to be maintained during transient N assimilation. This is consistent with N-induced photosynthetic suppression resulting in part from the severity of competition for carbon skeletons between the Calvin cycle and N assimilation.

Acknowledgments—We are grateful to Queen's University Visual Aids Centre for preparing the artwork. We wish to thank D. G. Birch, D. T. Canvin, S. Gaito, B. King, D. B. Layzell, K. B. Walsh, and G. Weagle for assistance with HPLC operation, numerical analysis and helpful comments.

LITERATURE CITED

1. BASSHAM JA, PO LARSEN, AL LAWYER, KL CORNWELL 1981 Relationships between nitrogen metabolism and photosynthesis. *In* JD Bewley, ed, Nitrogen and Carbon Metabolism. Junk, London, pp 135–163
2. BASSHAM JA, MR KIRK 1964 Photosynthesis of amino acids. Biochim Biophys Acta 90: 553–562
3. BIRCH DG, IR ELRIFI, DH TURPIN 1986 Nitrate and ammonium induced photosynthetic suppression in N-limited *Selenastrum minutum*. II. Effects of NO_3^- and NH_4^+ addition on CO_2 efflux in the light. Plant Physiol 82: 708–712
4. ELRIFI IR, DB LAYZELL, BJ KING, G WEAGLE, DH TURPIN 1986 Inexpensive, computer automated HPLC for ion-exchange separation and quantification of amino acids in physiological fluids. J Liq Chromatogr 9: 2199–2221
5. ELRIFI IR, DH TURPIN 1986 Nitrate and ammonium induced photosynthetic suppression in N-limited *Selenastrum minutum*. Plant Physiol 81: 273–279
6. GRANT BR, F WINKENBACH, DT CANVIN, RGS BIDWELL 1972 The effect of nitrate, nitrite, and ammonia on photosynthesis by *Acetabularia* chloroplast preparations compared with spinach chloroplasts and whole cells of *Acetabularia* and *Dunaliella*. Can J Bot 50: 2535–2543
7. GREENBERG DM, M ROTHSTEIN 1957 Methods for chemical synthesis, isolation and degradation of labeled compounds as applied in metabolic studies of amino acids and proteins. Methods Enzymol 4: 657–732
8. KANAZAWA T, K KANAZAWA, MR KIRK, JA BASSHAM 1970 Difference in nitrate reduction in 'light' and 'dark' stages of synchronously grown *Chlorella pyrenoidosa* and resultant metabolic changes. Plant Cell Physiol 11: 445–452
9. KANAZAWA T, MR KIRK, JA BASSHAM 1970 Regulatory effects of ammonia on carbon metabolism in photosynthesizing *Chlorella pyrenoidosa*. Biochim Biophys Acta 205: 401–408
10. KANAZAWA T, M DISTEFANO, JA BASSHAM 1983 Ammonia regulation of intermediary metabolism in photosynthesizing and respiring *Chlorella pyrenoidosa*: comparative effects of methylamine. Plant Cell Physiol 24: 979–986
11. LARSEN PO, KL CORNWELL, SL GEE, JA BASSHAM 1981 Amino acid synthesis in photosynthesizing spinach cells: effects of ammonia on pool sizes and rates of labeling from $^{14}CO_2$. Plant Physiol 68: 292–299
12. LAWRIE AC, GA CODD, WDP STEWART 1976 The incorporation of nitrogen into products of recent photosynthesis in *Anabaena cylindrica* Lemm. Arch Microbiol 107: 15–24
13. LAWYER AL, KL CORNWELL, PO LARSEN, JA BASSHAM 1981 Effects of carbon dioxide and oxygen on the regulation of photosynthetic carbon metabolism by ammonia in spinach mesophyll cells. Plant Physiol 68: 1231–1236
14. MARSH HV JR, JM GALMICHE, M GIBBS 1965 Effect of light on the tricarboxylic acid cycle in *Scenedesmus*. Plant Physiol 40: 1013–1021
15. MIFLIN BJ, PJ LEA 1980 Ammonia assimilation. *In* PK Stumpf, EE Conn, eds, The Biochemistry of Plants, Vol 5. Academic Press, New York pp 169–202
16. MIYACHI S, S MIYACHI 1985 Ammonia induces starch degradation in *Chlorella* cells. Plant Cell Physiol 26: 245–252
17. MOHAMED AH, A GNANAM 1979 A possible mechanism of ammonium ion

regulation of photosynthetic carbon flow in higher plants. Plant Physiol 64: 263–268
18. OHMORI M, A HATTORI 1978 Transient change in the ATP pool of *Anabaena cylindrica* associated with ammonia assimilation. Arch Microbiol 117: 17–20
19. OHMORI M, S MIYACHI, K OKABE, S MIYACHI 1984 Effects of ammonia on respiration, adenylate levels, amino acid synthesis and CO_2 fixation in cells of *Chlorella vulgaris* 11h in darkness. Plant Cell Physiol 25: 749–756
20. PAUL JS, KL CORNWELL, JA BASSHAM 1978 Effects of ammonia on carbon metabolism in photosynthesizing isolated mesophyll cells from *Papaver somniferum* L. Planta 142: 49–54
21. PLATT SG, Z PLAUT, JA BASSHAM 1977 Ammonia regulation of carbon metabolism in photosynthesizing leaf discs. Plant Physiol 60: 739–742
22. PREISS J 1984 Starch, sucrose biosynthesis and partition of carbon in plants are regulated by orthophosphate and triose phosphates. Trends Biochem Sci 9: 24–27
23. RECH J, J CROUZET 1974 Partial purification and initial studies of the tomato L-alanine:2-oxoglutarate aminotransferase. Biochim Biophys Acta 350: 392–399
24. RUTTER WJ, HA LARDY 1958 Purification and properties of pigeon liver malic enzyme. J Biol Chem 233: 374–382
25. SCHULZE-SIEBERT D, D HEINEKE, H SCHARF, G SCHULTZ 1984 Pyruvate derived amino acids in spinach chloroplasts: synthesis and regulation during photosynthetic carbon metabolism. Plant Physiol 76: 465–471
26. SHARKEY TD 1985 Photosynthesis in intact leaves of C3 plants: physics, physiology and rate limitations. Bot Rev 51: 53–105
27. SYRETT PJ 1956 The assimilation of ammonia and nitrate by nitrogen-starved cells of *Chlorella vulgaris*. IV. The dark fixation of carbon dioxide. Physiol Plant 9: 165–171
28. WALKER DA, MR SIVAK 1985 Can phosphate limit photosynthetic carbon assimilation *in vivo*. Physiol Veg 23: 829–841
29. WISKICH J 1980 Control of the Krebs cycle. *In* PK Stumpf, EE Conn, eds, The Biochemistry of Plants, Vol 2. Academic Press, New York, pp 244–278
30. WOO KC, DT CANVIN 1980 Effect of ammonia on photosynthetic carbon fixation in isolated spinach leaf cells. Can J Bot 58: 505–510